Arabidopsis Actin-Depolymerizing Factor AtADF4 Mediates Defense Signal Transduction Triggered by the *Pseudomonas syringae* Effector AvrPphB[1][W][OA]

Miaoying Tian, Faisal Chaudhry[2], Daniel R. Ruzicka[3], Richard B. Meagher, Christopher J. Staiger, and Brad Day*

Department of Plant Pathology, Michigan State University, East Lansing, Michigan 48824–1311 (M.T., B.D.); Department of Biological Sciences, Purdue University, West Lafayette, Indiana 47907–2064 (F.C., C.J.S.); and Department of Genetics, University of Georgia, Athens, Georgia 30602–7223 (D.R.R., R.B.M.)

The actin cytoskeleton has been implicated in plant defenses against pathogenic fungi and oomycetes with limited, indirect evidence. To date, there are no reports linking actin with resistance against phytopathogenic bacteria. The dynamic behavior of actin filaments is regulated by a diverse array of actin-binding proteins, among which is the Actin-Depolymerizing Factor (ADF) family of proteins. Here, we demonstrate that actin dynamics play a role in the activation of gene-for-gene resistance in Arabidopsis (*Arabidopsis thaliana*) following inoculation with the phytopathogenic bacterium *Pseudomonas syringae* pv *tomato*. Using a reverse genetics approach, we explored the roles of Arabidopsis ADFs in plant defenses. AtADF4 was identified as being specifically required for resistance triggered by the effector AvrPphB but not AvrRpt2 or AvrB. Recombinant AtADF4 bound to monomeric actin (G-actin) with a marked preference for the ADP-loaded form and inhibited the rate of nucleotide exchange on G-actin, indicating that AtADF4 is a bona fide actin-depolymerizing factor. Exogenous application of the actin-disrupting agent cytochalasin D partially rescued the *Atadf4* mutant in the AvrPphB-mediated hypersensitive response, demonstrating that AtADF4 mediates defense signaling through modification of the actin cytoskeleton. Unlike the mechanism by which the actin cytoskeleton confers resistance against fungi and oomycetes, AtADF4 is not involved in resistance against pathogen entry. Collectively, this study identifies AtADF4 as a novel component of the plant defense signaling pathway and provides strong evidence for actin dynamics as a primary component that orchestrates plant defenses against *P. syringae*.

The actin cytoskeleton has been implicated in plant defenses against pathogenic fungi and oomycetes (Hardham et al., 2007). Evidence largely comes from studies using actin cytoskeleton-disrupting agents, such as cytochalasins. Treatments with a variety of cytochalasins were shown to increase the penetration rate of both adapted and nonadapted pathogens in multiple plant-pathogen systems, thereby implicating the actin cytoskeleton as having a role in basal defenses and nonhost resistance (Kobayashi et al., 1997; Yun et al., 2003; Shimada et al., 2006; Miklis et al., 2007). The actin cytoskeleton may also play a role in race-specific resistance (Skalamera and Heath, 1998). To date, no reports linking actin dynamics with resistance against phytopathogenic bacteria have been published.

While the actin cytoskeleton as a virulence target of plant pathogens has not been documented, it was well characterized in mammalian pathosystems, particularly in studies investigating macrophage interactions with the pathogenic bacterium *Yersinia pestis* (Mattoo et al., 2007). *Yersinia* species deliver a suite of effectors into the target host cell, and at least four of them (YopE, YpkA/YopO, YopT, and YopH) are involved in rearrangement of the actin cytoskeleton (Aepfelbacher and Heesemann, 2001). YopT, a Cys protease, targets a plasma membrane-localized Rho GTPase in affected phagocytes (Aepfelbacher and Heesemann, 2001). Cleavage of the GTPase by YopT releases the prenylated protein from the plasma membrane and disrupts the actin cytoskeleton, effectively shutting down phagocytosis, preventing elimination of the pathogen (Iriarte and Cornelis, 1998; Shao et al., 2002). Similarly, microbial pathogens also usurp host processes for the

[1] This work was supported by the National Science Foundation (CAREER Award no. IOB–0641319 to B.D.), by Michigan State University (Vice President for Research and Graduate Studies Intramural Research Grants Program award) and the Michigan Agricultural Experiment Station (to B.D.), by the Department of Energy-Energy Biosciences Division (grant no. DE–FG02–04ER15526) and the National Research Initiative Competitive Grants Program of the U.S. Department of Agriculture (grant no. 2002–35304–12412) to C.J.S., and by the National Institutes of Health (grant no. GM 36397–21) to R.M.

[2] Present address: Rosenstiel Center MS 029, Brandeis University, Waltham, MA 02454.

[3] Present address: Donald Danforth Plant Science Center, St. Louis, MO 63132.

* Corresponding author; e-mail bday@msu.edu.

The author responsible for distribution of materials integral to the findings presented in this article in accordance with the policy described in the Instructions for Authors (www.plantphysiol.org) is: Brad Day (bday@msu.edu).

[W] The online version of this article contains Web-only data.

[OA] Open Access articles can be viewed online without a subscription.

www.plantphysiol.org/cgi/doi/10.1104/pp.109.137604

benefit of infection, disease, and death. *Listeria* species hijack the host's cytoskeleton to move around inside the infected cell through the induction of directed polymerization of actin (Pistor et al., 1994). *Salmonella* injects into host cells two actin-binding proteins (SipA and SipC) as well as other regulators of actin dynamics to enhance phagocytic uptake and intracellular propagation (Galan and Zhou, 2000). In short, either by preventing polymerization or by promoting it, pathogens have evolved strategies to modify the host actin cytoskeleton for purposes of evading detection or eliciting disease and death.

Dynamic actin cytoskeleton rearrangements are regulated by a pool of actin-binding proteins, which sense environmental changes and modulate the cytoskeleton through various biochemical activities (Hussey et al., 2006; Staiger and Blanchoin, 2006). Among the proteins that regulate these dynamic processes are the Actin-Depolymerizing Factor (ADF) family of proteins (Maciver and Hussey, 2002). In general, ADFs bind both monomeric (G-) and filamentous (F-) actin to increase actin dynamics. They function by severing F-actin to generate more ends for polymerization and by increasing the dissociation rate of actin monomers from the pointed ends (Maciver, 1998; Maciver and Hussey, 2002). Plant ADFs play roles in pollen tube growth (Chen et al., 2003), root formation (Thomas and Schiefelbein, 2002), and cold acclimation (Ouellet et al., 2001). There is also one report linking ADFs with plant defenses (Miklis et al., 2007). In that study, ectopic expression of barley (*Hordeum vulgare*) HvADF3 and several isovariants of Arabidopsis (*Arabidopsis thaliana*) ADFs in barley epidermal cells was shown to compromise penetration resistance to powdery mildew fungi (Miklis et al., 2007).

The Arabidopsis-*Pseudomonas syringae* interaction provides an ideal model plant-pathogen system to study plant defense signaling. Like *Yersinia* species, *P. syringae* delivers effector proteins into the host cells via the type III secretion system and relies on these proteins for pathogenesis (Alfano and Collmer, 2004). However, once these proteins (Avr) are recognized either directly or indirectly by plant resistance (R) proteins, plant immune responses are activated (Jones and Dangl, 2006). Exciting progress has been made toward understanding the indirect recognition of several pairs of Avr-R proteins; the best examples include AvrB/AvrRPM1-RPM1, AvrRpt2-RPS2, and AvrPphB-RPS5. During activation of defense mediated by AvrB/AvrRPM1-RPM1 and AvrRpt2-RPS2, the phosphorylation or elimination of a third protein, RIN4, is essential (Mackey et al., 2002; Axtell and Staskawicz, 2003). In the case of AvrPphB-RPS5 recognition, the AvrPphB Cys protease of the same family as YopT (Shao et al., 2002) cleaves the plant protein kinase PBS1, inducing a conformational change in RPS5, which in turn leads to the activation of resistance (Ade et al., 2007). Although these studies have greatly enhanced our understanding of how pathogen effectors initiate plant defense responses, the ultimate signaling processes associated with the activation of resistance remain largely unknown, due to the limited number of genetic loci identified in these pathways. In this work, we hypothesize that actin-binding proteins play a role during plant-bacteria interactions based on the functional and structural similarity between AvrPphB and YopT.

There are 11 ADFs in the Arabidopsis genome (Ruzicka et al., 2007). We utilized a reverse genetics approach to identify the putative roles these proteins play in plant resistance against the bacterial pathogen *P. syringae* pv *tomato* (*Pst*). AtADF4 was identified as a novel signaling component in the AvrPphB-RPS5-mediated defense signal transduction pathway. Loss of AtADF4 confers on Arabidopsis enhanced susceptibility to *P. syringae* expressing AvrPphB. Further subcellular localization and biochemical analyses, as well as pharmacological studies, suggest that AtADF4 functions as a bona fide actin-depolymerizing factor through modifying the actin cytoskeleton. Unlike the documented mechanism by which the actin cytoskeleton plays roles in resistance against fungi and oomycetes, the resistance against *P. syringae* mediated by AtADF4 is not involved in hindering pathogen entry.

RESULTS

The *Atadf4* Knockout Mutant Specifically Compromises AvrPphB-Mediated Resistance against *Pst*

To identify a role for the Arabidopsis ADFs in plant defenses, we obtained and characterized 14 T-DNA insertion lines corresponding to AtADF1, AtADF2, AtADF3, AtADF4, AtADF5, and AtADF9 (Supplemental Table S1). Four lines (Salk_144459, Salk_139265, Garlic_823_A11.b.1b.Lb3Fa, and Salk_056064) were confirmed to be null mutants and were named *Atadf1*, *Atadf3*, *Atadf4*, and *Atadf9* (Fig. 1B; Supplemental Fig. S1). Homozygous mutant plants were dip inoculated with the *Pst* DC3000 virulent strain as well as three avirulent strains expressing AvrRpt2, AvrB, and AvrPphB. Multiple independent experiments showed that *Atadf1*, *Atadf3*, *Atadf4*, and *Atadf9* responded similar to wild-type ecotype Columbia (Col-0) upon inoculation with the virulent strain as well as strains expressing AvrRpt2 and AvrB (Fig. 1C; data not shown). However, in response to inoculation with *Pst* expressing AvrPphB, the *Atadf4* mutant, which contains a T-DNA insertion at the second exon (Fig. 1A), was strikingly more susceptible than the wild type and the other *Atadf* mutant plants (Fig. 1C). Quantitative analysis of bacterial growth revealed that infected leaves of *Atadf4* supported a significantly larger bacterial population than wild-type plants infected with *Pst* expressing AvrPphB (Fig. 1D).

Since the hypersensitive response (HR) is typically associated with gene-for-gene resistance, we further tested the *Atadf* mutant lines for induction of the HR in response to inoculation with the *Pst* strains described

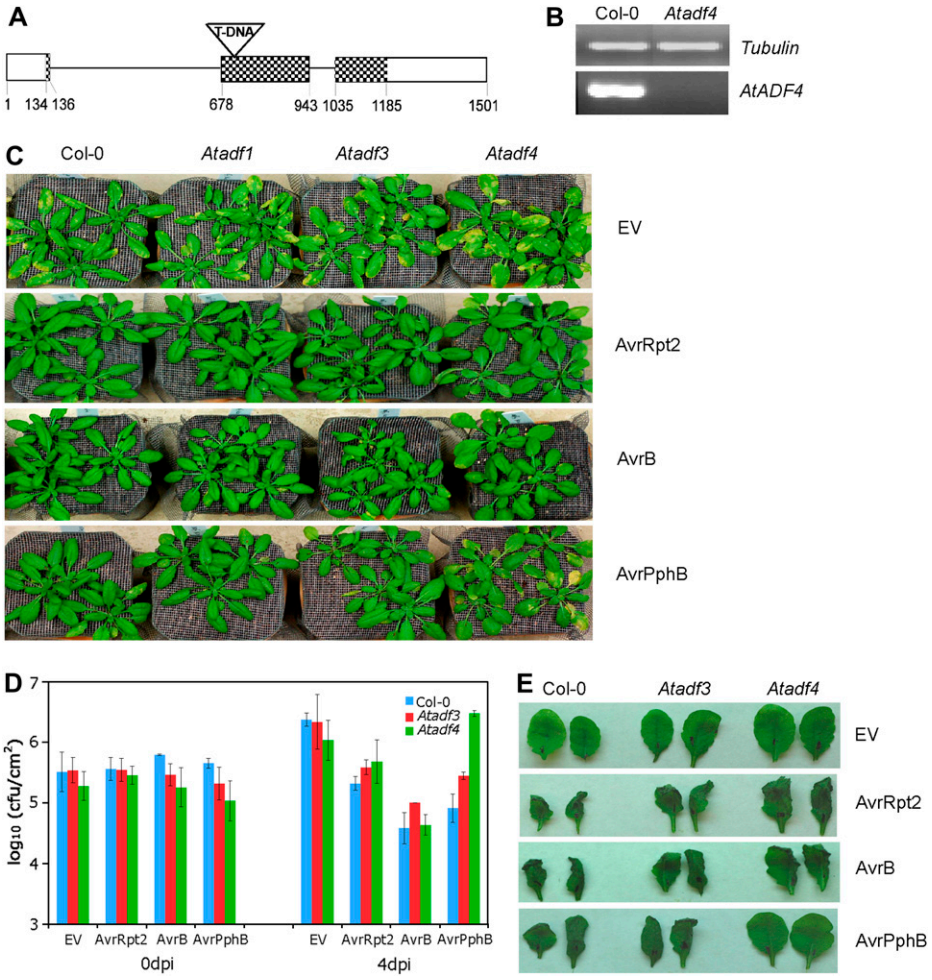

Figure 1. The *Atadf4* mutant compromises AvrPphB-mediated resistance against *Pst*. A, Diagram of the *AtADF4* gene carrying a T-DNA insertion in the second exon, from the 5′ untranslated region to the 3′ untranslated region. Introns and exons are shown as thick lines and boxes, respectively. Shaded boxes represent protein-encoding sequences. The numbers indicate nucleotide positions. B, RT-PCR analysis of *AtADF4* gene expression. Amplification of the *β-tubulin* gene was used as an endogenous control. For resistance analysis, Col-0 and *Atadf* mutant plants were inoculated with *Pst* expressing empty vector (EV), AvrRpt2, AvrB, and AvrPphB. C, Disease phenotypes at 4 d after dip inoculation. D, Bacterial populations at 0 and 4 d after dip inoculation (dpi). Error bars represent SE values calculated from three replications. E, HR at 22 h after bacteria infiltration. Two representative leaves of 12 infiltrated from four plants are shown. All experiments were repeated at least three times.

above. As expected, leaves from wild-type plants developed the HR upon infiltration with three avirulent strains after 18 to 22 h, yet not after inoculation with the virulent strain (Fig. 1E). There was no difference between the four *Atadf* mutant lines and wild-type plants in response to the virulent strain and strains expressing AvrRpt2 and AvrB (Fig. 1E; data not shown). However, the *Atadf4* mutant specifically suppressed the HR mediated by *Pst* expressing AvrPphB (Fig. 1E).

Infection of plants by *Pst* involves antagonistic cross talk between salicylic acid (SA)- and jasmonic acid (JA)-dependent signaling pathways, and the plant susceptibility is associated with induction of JA-responsive genes and concomitant repression of SA-responsive pathogenesis-related (PR) genes (Zhao et al., 2003). We tested the gene expression of *PR1* and *PDF1.2*, marker genes for the SA and JA pathways, respectively, during the infection time course after wild-type and *Atadf4* mutant plants were dip inoculated with *Pst* expressing AvrPphB. Consistent with the compromised resistance phenotype of the *Atadf*4 mutant in response to *Pst* expressing AvrPphB, *PR1* gene expression of *Atadf4* was delayed and reduced compared with the wild type (Fig. 2A), while *PDF1.2* expression was highly elevated (Fig. 2B). The induction of the JA signaling pathway in *Atadf4* was independently confirmed with microarray data collected at 24 h after dip inoculation. Among 23 differentially expressed JA-responsive genes, 22 of them were up-regulated in *Atadf4* compared with the wild type (M. Tian and B. Day, unpublished data).

Silencing of Four *AtADF*s Uncouples the AvrPphB-Triggered HR from Resistance

To obtain additional evidence that Arabidopsis ADFs are required for AvrPphB-mediated resistance, and to determine whether the Arabidopsis ADFs play redundant roles in resistance mediated by other effectors, we generated the gene-silencing construct *AtADF1-4Ri*, which simultaneously targets all four subclass I *ADF*s, *AtADF1* through *AtADF4* (Ruzicka et al., 2007). Four independent homozygous lines were tested by quantitative RT-PCR to determine the expression level of each of the *AtADF* genes. The gene expression of these four genes in all four transgenic *AtADF1-4Ri* lines was reduced when compared with

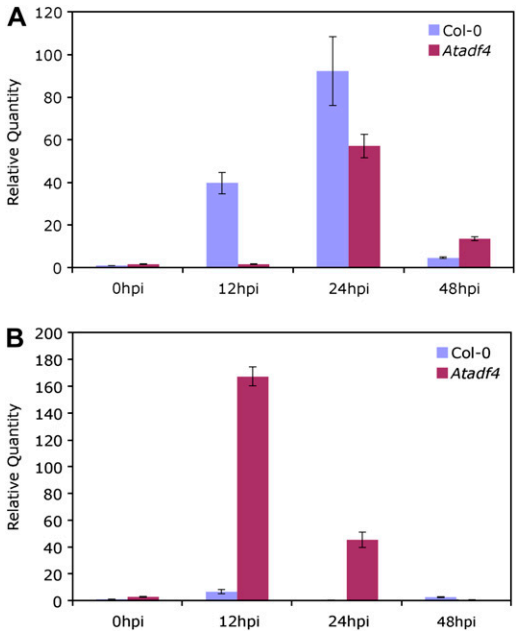

Figure 2. Relative transcript levels of *PR1* (A) and *PDF1.2* (B) in Col-0 and the *Atadf4* mutant during the infection time course after dip inoculation with *Pst* DC3000 expressing AvrPphB, determined by quantitative RT-PCR, with amplification of *UBQ10* as an endogenous control. The transcript levels of *PR1* and *PDF1.2* in Col-0 at 0 h after inoculation (hpi) were set to 1. Similar results were obtained from two biological replicates. Error bars represent SD values from three technical replicates of one biological replicate.

wild-type plants (Fig. 3A). HR tests were performed as described above. As we observed with the *Atadf4* T-DNA insertion mutant, all four knockdown lines specifically suppressed the HR mediated by AvrPphB but not other effectors (Fig. 3B; data not shown), suggesting that AtADF(s) are required for the AvrPphB-mediated HR. We further investigated the disease resistance phenotype(s) of these lines by dip inoculation. Interestingly, silencing of the four *AtADF*s did not result in a detectable loss of resistance. All four *AtADF1-4Ri* lines exhibited resistant phenotypes similar to that of wild-type plants, and none of them supported significantly more bacterial growth than wild-type plants for all strains tested (data not shown).

The *AtADF4* Gene Complements the *Atadf4* Knockout Mutant

Although the experiments described above suggested that AtADF4 is likely involved in AvrPphB-mediated resistance, they did not determine whether AtADF4 itself is required for defense signaling. To test this hypothesis, we transformed the homozygous *Atadf4* mutant plants with a construct expressing *AtADF4* genomic DNA fused with a C-terminal T7 tag, driven by the *AtADF4* native promoter. T3 plants from two independent homozygous transgenic lines did not exhibit the disease phenotype as observed with the *Atadf4* mutant following inoculation with *Pst* expressing AvrPphB (Fig. 4A). Further measurements of bacterial growth were consistent with the resistant phenotype, as these two lines supported bacterial populations equivalent to those observed in wild-type plants (Fig. 4B). These data strongly support our finding that *AtADF4* is able to restore the resistance compromised in the *Atadf4* mutant. Similarly, using the HR as a second test for the activation of resistance, *AtADF4*-complemented lines showed a restoration in the activation of the HR (Fig. 4C). The integrity of the transgenic lines was also tested; results of these analyses are shown in Supplemental Figure S2. Taken together, the complementation experiments provide strong evidence that AtADF4 is an essential signaling component of the AvrPphB-mediated resistance transduction pathway.

AtADF4 Is Localized on the Actin Cytoskeleton

To determine the subcellular localization of AtADF4, a DsRed-AtADF4 fusion protein was transiently expressed in *Nicotiana benthamiana* and protein localization was determined using confocal microscopy. In contrast to DsRed alone (Fig. 5A), DsRed-AtADF4 is localized in a filamentous pattern (Fig. 5B), suggesting that AtADF4 is associated with the cytoskeleton. To further confirm that AtADF4 is localized along actin filaments, we coexpressed DsRed-AtADF4 with GFP-labeled ABD2, the second actin-binding domain of Arabidopsis Fimbrin1, which was developed as a reporter of the actin cytoskeleton (Wang et al., 2004). As expected, the green fluorescence of ABD2-GFP substantially overlapped with the red fluo-

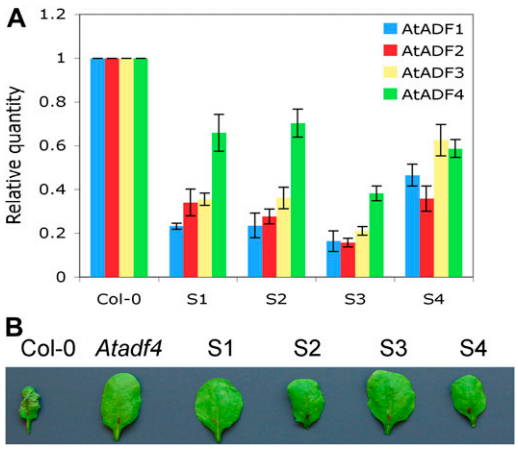

Figure 3. *AtADF* gene-silencing lines suppress the AvrPphB-mediated HR. A, Relative quantity of transcripts for *AtADF* genes in four independent transgenic lines (S1, S2, S3, and S4), determined by quantitative RT-PCR, with amplification of *UBQ10* gene as an endogenous control. Error bars represent SD values from three replicates. B, HR at 22 h after inoculation with *Pst* expressing AvrPphB. One representative leaf of 12 inoculated from four plants is shown. Experiments were repeated three times.

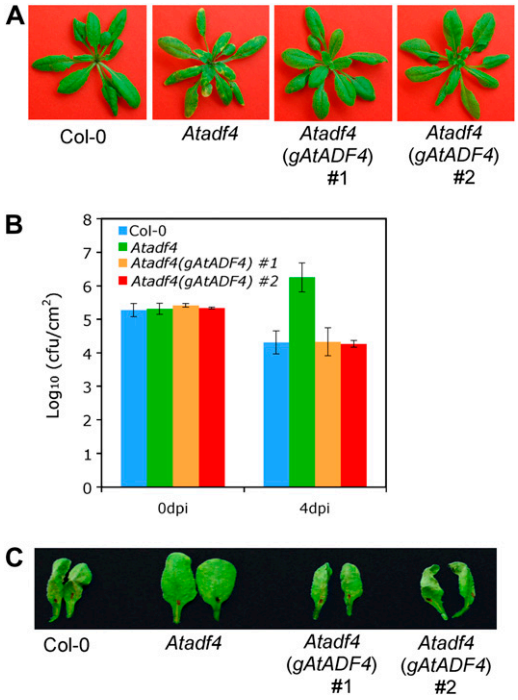

Figure 4. *AtADF4* genomic DNA complements the *Atadf4* mutant for resistance against *Pst* expressing AvrPphB. A, Disease phenotypes at 4 d after dip inoculation. B, Bacterial populations at 0 and 4 d after dip inoculation (dpi). Error bars represent SE values calculated from three replications. C, HR at 22 h after bacteria infiltration. Two representative leaves of 12 infiltrated from four plants are shown. *Atadf4* (*gAtADF4*) #1 and #2 represent two independent transgenic lines. Experiments were repeated three times.

rescence of DsRed-AtADF4 (Fig. 5, F–H) but not with DsRed alone (Fig. 5, C–E), demonstrating that AtADF4 is localized on the actin cytoskeleton. Note that sometimes the actin cytoskeleton appears slightly perturbed (Fig. 5, F–H), which is not surprising given that AtADF1 overexpression has been shown previously to reduce the extent of actin bundles in Arabidopsis cells (Dong et al., 2001).

AtADF4 Shows a Marked Preference for ADP-G-Actin

ADFs from diverse organisms generally share the ability to bind G-actin, with higher affinity for ADP-G-actin versus ATP-G-actin (Carlier et al., 1999). For example, AtADF1 shows approximately 100-fold higher affinity for ADP-G-actin when compared with ATP-loaded monomer (Carlier et al., 1997; Chaudhry et al., 2007). To test the activities of AtADF4, we purified recombinant AtADF4 protein fused with an N-terminal FLAG tag. The protein, which migrated as a single approximately 17-kD polypeptide on SDS-PAGE gels (Fig. 6A), was used for G-actin-binding assays as well as for nucleotide-exchange experiments described below. AtADF1, expressed and purified from *Escherichia coli* as described previously (Carlier et al., 1997; Chaudhry et al., 2007), was used as a control. The affinity of AtADF4 for ATP- and ADP-G-actin was tested with 7-chloro-4-nitrobenzo-2-oxa-1,3-diazole (NBD)-labeled actin. A dose-dependent quenching of fluorescence for 0.2 μM NBD-G-actin was observed in the presence of both Arabidopsis ADF isoforms. As shown in Figure 6B, the quenching of NBD-G-actin fluorescence was maximal when 12 to 18 μM AtADF1 was added to ATP-G-actin, whereas AtADF4 failed to reach saturation at these concentrations. In marked contrast, the quenching of NBD fluorescence on ADP-G-actin was maximal when ADF1 or ADF4 concentration was above 2 μM (Fig. 6C). From several such experiments, average dissociation constant (K_d) values ($\pm$SD [n]) of 37 $\pm$ 9 μM (3) for AtADF4 binding to ATP-G-actin and 0.104 $\pm$ 0.04 μM (4) for AtADF4 binding to ADP-G-actin were determined. AtADF1 gave average K_d values of 16 $\pm$ 3 μM (4) for ATP-actin and 0.216 $\pm$ 0.112 μM (4) for ADP-actin, in agreement with published data (Carlier et al., 1997; Chaudhry et al., 2007). Therefore, AtADF4 has approximately 355-fold higher affinity for ADP-G-actin when compared with the ATP-loaded form.

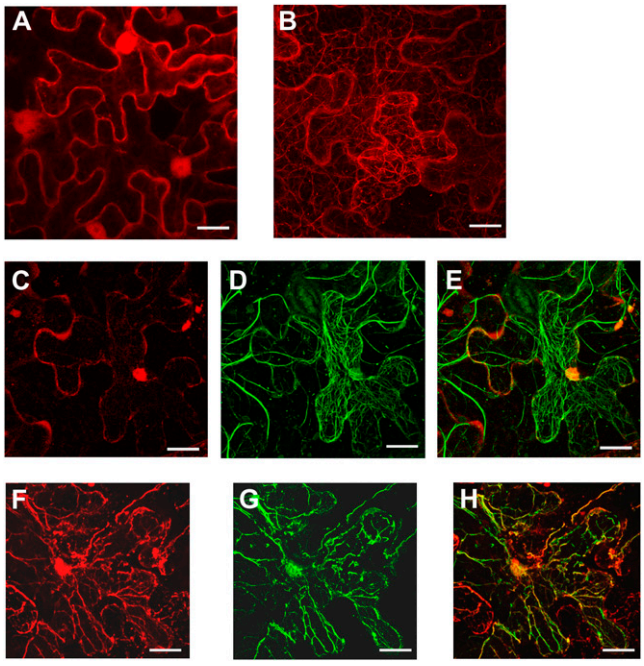

Figure 5. Laser-scanning confocal micrographs showing fluorescence of leaf cells expressing DsRed alone (A), DsRed-AtADF4 alone (B), coexpressing DsRed and ABD2-GFP (C–E), or coexpressing DsRed-AtADF4 and ABD2-GFP (F–H). The red channel shows localization of DsRed alone (A, C, and E) or DsRed-AtADF4 (B, F, and H). The green channel shows localization of ABD2-GFP (D, E, G, and H). E shows an overlay of micrographs from C and D. H shows an overlay of micrographs of F and G. Bars = 20 μm.

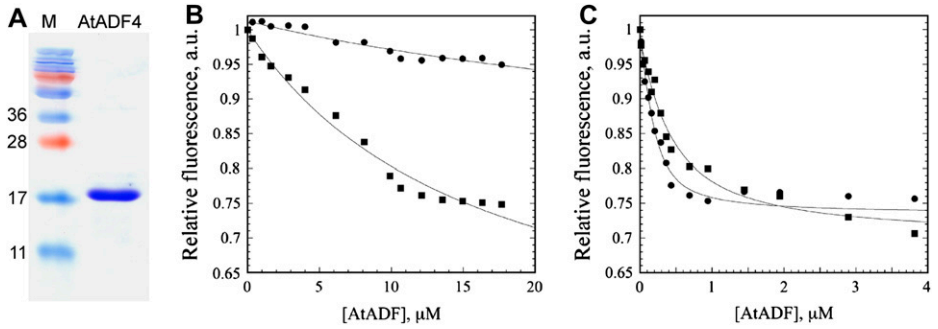

Figure 6. AtADF4 binds with higher affinity to ADP-G-actin than to ATP-G-actin. A, SDS-PAGE gel of the purified recombinant protein AtADF4 with an N-terminal FLAG tag. The numbers on the left indicate the molecular masses of the marker proteins in kD. B, Binding to ATP-G-actin was followed by quenching of NBD-actin fluorescence in the presence of varying amounts of AtADF1 (squares) and AtADF4 (circles). This single representative experiment allowed estimation of K_d values of 16 and 44 μM for AtADF1 and AtADF4, respectively. C, The binding of AtADF1 and AtADF4 to NBD-labeled ADP-G-actin, from a single representative experiment, gave K_d values of 0.3 and 0.08 μM, respectively. a.u., Arbitrary fluorescence units.

AtADF4 Inhibits the Rate of Nucleotide Exchange on G-Actin

Nucleotide exchange analysis using 1 μM ATP-G-actin in the presence or absence of AtADFs, under both physiological and low-salt conditions, was performed. Under low-salt conditions, the rate of nucleotide exchange in the presence of 2.5 or 5 μM AtADF4 was significantly lower than for ATP-G-actin alone (Fig. 7A). Nucleotide exchange in the presence of 1 μM AtADF1 was used as a positive control. However, with a physiological ionic strength buffer, no inhibition was observed even in the presence of 10 μM AtADF4 or AtADF1 (data not shown). Given the weak binding affinity of AtADF4 for ATP-G-actin, we decided to monitor nucleotide exchange on 1 μM ADP-G-actin under physiological salt conditions. In agreement with previously published findings using other ADF proteins (Ouellet et al., 2001; Chaudhry et al., 2007), AtADF4 markedly inhibited the rate of nucleotide exchange in a concentration-dependent manner (Fig. 7B). Thus, AtADF4 shows two conserved biochemical features of eukaryotic ADF proteins: the ability to bind monomeric actin with a marked preference for the ADP-loaded form and the ability to inhibit nucleotide exchange on monomers. Preliminary results indicate that AtADF4 also binds filamentous actin and induces severing (data not shown).

Cytochalasin D Partially Rescues the *Atadf4* Mutant in the AvrPphB-Mediated HR

To gain insight into AtADF4's role in transducing defense signaling through its action on the actin cytoskeleton, we coinfiltrated cytochalasin D with *Pst* DC3000 expressing AvrPphB into leaves of wild-type and *Atadf4* mutant plants and measured the effects on induction of the HR. Cytochalasin D was applied at varying concentrations in combination with and without coinoculation with *Pst*. As expected, application of cytochalasin D alone did not result in tissue collapse, nor did increasing the concentration of cytochalasin D in coinoculation experiments with bacterial suspensions affect the induction of the HR in wild-type plants (Table I). Interestingly, exogenously applied cytochalasin D restored a significant percentage of leaves from the *Atadf4* mutant to generate the HR (Table I). The average proportion of leaves developing an HR was

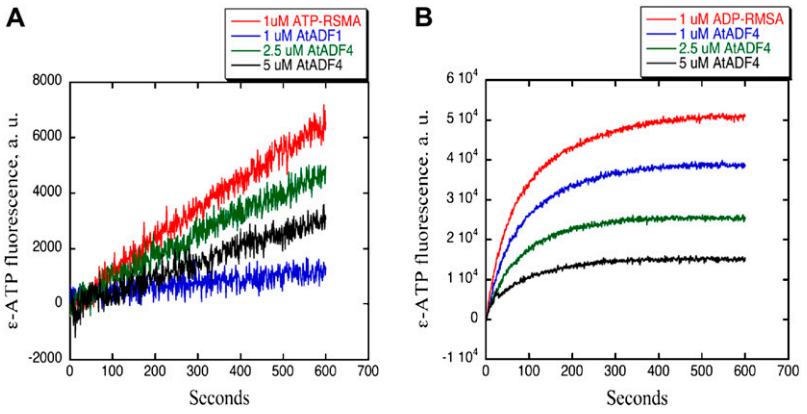

Figure 7. AtADF4 inhibits nucleotide exchange on rabbit skeletal muscle actin (RSMA). A, Nucleotide exchange on 1 μM ATP-G-actin under low-ionic-strength conditions. B, Nucleotide exchange on 1 μM ADP-G-actin under physiological ionic conditions. A concentration of 1 μM ATP(ADP)-RSMA represents nucleotide exchange in the absence of AtADFs. a.u., Arbitrary fluorescence units.

Table I. *Effects of cytochalasin D on the HR of the Atadf4 mutant triggered by AvrPphB*
CD, Cytochalasin D; n/d, not determined.

Treatment	No. of Leaves with HR/Total No. of Leaves					
	Experiment 1		Experiment 2		Experiment 3	
	Col-0	*Atadf4*	Col-0	*Atadf4*	Col-0	*Atadf4*
Pst DC3000 (empty vector)	0/12	0/11	0/9	0/10	0/11	0/10
Pst DC3000 (AvrPphB)	13/13	0/12	8/8	0/11	12/12	0/11
2.5 μM CD	n/d	n/d	0/10	0/8	0/12	0/12
5 μM CD	n/d	n/d	0/9	0/13	0/13	0/11
10 μM CD	0/10	0/12	0/11	0/13	0/11	0/9
Pst DC3000 (AvrPphB) + 0.1% DMSO	12/12	0/12	8/8	0/9	10/10	0/11
Pst DC3000 (AvrPphB) + 2.5 μM CD	n/d	n/d	8/8	7/13	11/11	5/11
Pst DC3000 (AvrPphB) + 5 μM CD	12/12	10/14	13/13	9/12	12/12	4/14
Pst DC3000 (AvrPphB) + 10 μM CD	11/11	5/12	12/12	3/10	11/11	5/15

49.6%, 58.3%, and 35% for concentrations of 2.5, 5, and 10 μM cytochalasin D, respectively. This result strongly supports the hypothesis that AtADF4 transduces defense signaling through modification of the actin cytoskeleton.

AtADF4 Is Not Involved in Resistance against Bacterial Entry

So far, the documented mechanism for actin cytoskeleton-based resistance is to hinder pathogen penetration (Hardham et al., 2007; Miklis et al., 2007). To determine if AtADF4 is also involved in penetration resistance, we tested the plant resistance of *Atadf* mutants after manually infiltrating *Pst* DC3000 strains into the extracellular space of the plants. Repeated experiments showed that *Atadf1*, *Atadf3*, and *Atadf4* responded similarly to wild-type plants upon inoculation with the virulent strain as well as strains expressing AvrRpt2 and AvrB (Fig. 8). However, in response to inoculation with *Pst* expressing AvrPphB, the *Atadf4* mutant supported a significantly larger bacterial population than wild-type and other *Atadf* mutant plants (Fig. 8). This is consistent with the result obtained by dip inoculation (Fig. 1D), suggesting that AtADF4 is not involved in resistance against bacterial entry.

DISCUSSION

The involvement of the actin cytoskeleton in plant resistance against pathogenic fungi and oomycetes is largely based on two lines of indirect evidence. First, studies using actin cytoskeleton-disrupting agents or the ectopic expression of ADFs show that plant resistance is compromised following pathogen inoculation (Kobayashi et al., 1997; Yun et al., 2003; Shimada et al., 2006; Miklis et al., 2007). Second, cytological studies have shown that the cytoplasm and nucleus are relocalized directly beneath the infection sites by the actin cytoskeleton machinery (Takemoto et al., 2003; Takemoto and Hardham, 2004). In this study, we determined that AtADF4 is required for AvrPphB-mediated resistance against the phytopathogenic bacterium *Pst*. Subcellular localization and biochemical analyses demonstrate that AtADF4 is a bona fide actin-binding protein possessing activities consistent with previously characterized ADFs. Further pharmacological studies suggest that AtADF4 mediates defense signaling via modification of the actin cytoskeleton. Our data also suggest that AtADF4 is not involved in resistance against bacterial entry. In total, this study provides strong evidence that the actin cytoskeleton plays an important role in the plant defenses against the phytopathogenic bacterium *P. syringae*, with a distinct mechanism from the one by which the actin cytoskeleton confers resistance against fungi and oomycetes.

Although the *AtADF1-4Ri* gene-silencing lines suppressed the AvrPphB-mediated HR, they retained the disease resistance phenotype. This finding is intriguing. First, it provides another piece of evidence that the

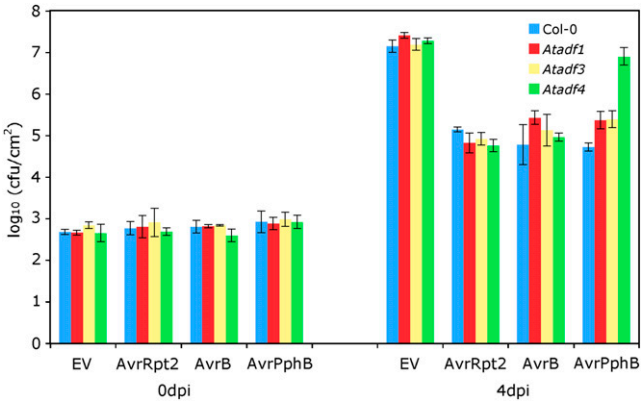

Figure 8. Bacterial populations of Col-0 and *Atadf* mutant plants at 0 and 4 d after hand infiltration (dpi) with 10^5 cfu mL^{-1} *Pst* DC3000 expressing empty vector (EV), AvrRpt2, AvrB, or AvrPphB. Error bars represent SE values calculated from three replications. Experiments were repeated twice.

HR can be uncoupled from resistance. This is consistent with previous studies showing that the HR is not always required for gene-for-gene resistance. Examples include the Arabidopsis *ndr1* and *dnd1* mutants. The *dnd1* mutant confers gene-for-gene disease resistance in the absence of HR (Yu et al., 1998). In the case of the *ndr1* mutant plants, while they compromise disease resistance triggered by AvrRPM1 and AvrB, they still exhibit HR-like lesions in response to high doses of bacterial inoculation (Century et al., 1995). Second, it suggests that AtADF4 might function in a dose-dependent manner to amplify the defense signal. Based on the hypothesis described by Jones and Dangl (2006), effective resistance, or the HR, is achieved only when the amplitude of the defense signal reaches a certain threshold; it is hypothesized that the threshold for eliciting the HR is higher than that for eliciting effective resistance. In the *AtADF* knockdown lines, it is possible that the residual transcript (and protein) levels are sufficient to sustain disease resistance yet insufficient to amplify the signal to attain the threshold for eliciting the HR.

One interesting question raised from our study is that of the functional specificity of AtADF isovariants. While AtADF4 was found to be required for AvrPphB-mediated resistance, it seems that AtADF1, AtADF3, and AtADF9 individually are dispensable. Ruzicka et al. (2007) classified the Arabidopsis ADFs into four subclasses. AtADF9 belongs to subclass III, whereas AtADF1, AtADF3, and AtADF4 belong to subclass I. The expression patterns of AtADF1 and AtADF3 were found to be similar to that observed for AtADF4; all are strongly expressed in most tissues and organs, with the exception of pollen (Ruzicka et al., 2007). From this, we can likely rule out the possibility that tissue-specific expression accounts for the differential phenotypes we observed in *Atadf1*, *Atadf3*, and *Atadf4* mutant lines upon infection with *P. syringae* expressing AvrPphB. Further studies investigating the differential gene expression patterns in response to pathogen inoculation, biochemical activities, as well as post-translational regulation may reveal the mechanisms determining this specificity.

The mechanism by which AtADF4 mediates AvrPphB-triggered resistance remains unknown. The simplest hypothesis is that AtADF4 is involved in the proper localization of proteins, a process in which the actin cytoskeleton is thought to play essential roles (Stamnes, 2002). During the infection of plants by pathogens, a wide range of effector proteins and/or cognate resistance proteins are collectively targeted (or relocalized) to various host cellular compartments, including the apoplast, plasma membrane, cytoplasm, and nucleus (Alfano and Collmer, 2004; Kamoun, 2007). In support of a role for the actin cytoskeleton in this process of dynamic protein relocalization following pathogen perception and defense activation, a recent study on tobacco mosaic virus effector p50 and its tobacco (*Nicotiana tabacum*) N receptor suggests that pathogen elicitor recognition defense signaling involves complex multistep processes at multiple subcellular compartments (Burch-Smith et al., 2007). This study indicates that the recognition of p50 by N protein likely occurs in the cytoplasm, and subsequent signaling is initiated by the activated N protein within the nucleus. Another example of dynamic protein relocalization processes associated with defense signaling in plants involves the immune receptor MLA10 and the effector AVR_{A10} from the powdery mildew fungus *Blumeria graminis* f. sp. *hordei* (Shen et al., 2007). Although the exact mechanisms remain unknown, it appears that the initiation of effector-triggered immunity involves active intracellular protein transport. In the case of AvrPphB and RPS5, the initial recognition is believed to take place at the plasma membrane (Nimchuk et al., 2000; Holt et al., 2005). Whether the activation of defense signaling requires relocalization of RPS5 to a second cellular compartment is not known, but it remains a possibility. Thus, AtADF4-mediated rearrangement of the actin cytoskeleton might be responsible for the transport of AvrPphB and RPS5 within the plasma membrane, or alternatively, away from the plasma membrane following the initial recognition events. Further localization studies of AvrPphB and RPS5 in both wild-type and *Atadf4* plants may shed light on this possibility.

An alternative hypothesis is that AtADF4 is directly involved in defense signal transduction. Although the mechanism is not fully understood, there is evidence showing that actin depolymerization itself may serve as a signal transducer. Studies on human B-cell receptor (BCR) signal transduction have shown that actin depolymerization enhances BCR-induced transcription factor activation. This finding suggests that by blocking actin depolymerization, BCR signaling is inhibited (Hao and August, 2005). A recent study also reported that depolymerization of the actin cytoskeleton in tobacco plants induces expression of the defense-related genes *PR1* and *PR2* (Kobayashi and Kobayashi, 2007). Similarly, actin depolymerization mediated by AtADF4 might directly transduce downstream defense signaling.

MATERIALS AND METHODS

Plants, Growth Conditions, and Arabidopsis Transformation

Arabidopsis (*Arabidopsis thaliana*) and *Nicotiana benthamiana* plants were grown at 20°C under a 14-h-light/10-h-dark cycle. Arabidopsis T-DNA insertion lines were obtained from the Arabidopsis Biological Resource Center. Arabidopsis transformation and selection of transformants were carried out as described by Clough and Bent (1998).

Pathogens, Inoculation, and Measurement of Bacterial Growth

Pseudomonas syringae pv *tomato* DC3000 strains containing pVSP61 (empty vector), AvrRpt2, AvrB, or AvrPphB (in the vector pVSP61) were described previously (Kunkel et al., 1993; Simonich and Innes, 1995). Four-week-old plants were used for bacterial infection. Dip inoculation was performed by dipping whole plants into bacterial suspensions of 3×10^8 colony-forming units (cfu) mL^{-1} as described by Kunkel et al. (1993). Hand infiltrations were

conducted with bacteria resuspended in 10 mM $MgCl_2$ to 5×10^7 cfu mL^{-1} for testing the HR or to 10^5 cfu mL^{-1} for measurement of bacterial growth. Before inoculation, three leaves of similar size from each plant were marked for analysis. To analyze the HR, leaves were scored for tissue collapse 20 to 24 h after inoculation. For measurement of bacterial growth, three leaf discs with a diameter of 0.7 cm were collected from three plants and placed into a single tube, serving as one replicate. Following bacteria recovery, serial dilution and plating were performed as described previously (Tornero and Dangl, 2001) with minor modifications. Instead of 2-μL drops, we plated 5-μL drops from each dilution on the plate for bacterial colony counting.

Plasmid Construction

Plasmid pFLAG-AtADF4 was constructed by cloning PCR-amplified AtADF4 protein-encoding sequence into *Hin*dIII and *Kpn*I sites of pFLAG-ATS (Sigma-Aldrich), a vector that allows secreted expression of N-terminally FLAG-tagged proteins in *Escherichia coli*. The primers 5′-GCGAAGCTTatggctaatgctgcgtcaggaatgg-3′ (forward) and 5′-GCGGGTACCttagttgacgcggcttttcaaaac-3′ (reverse) were used to amplify the fragment. The gene-specific sequence is shown in lowercase letters, and the introduced restriction sites are underlined. pGDR-AtADF4 was constructed by cloning AtADF4 protein-encoding sequence into *Bgl*II and *Sal*I sites of pGDR (Goodin et al., 2002). The primers used contain the same gene-specific sequence as above. To construct pMD1-gAtADF4, a genomic DNA fragment starting from 665 bp upstream of the AtADF4 start codon (e.g. ATG) to the stop codon TAA, was cloned into the binary vector pMD1(Li et al., 1997), which was digested with *Hin*dIII and *Xba*I to remove 35S promoter. Primers 5′-GCGAAGCTTacatcttgtcttcacataatgaaaac-3′ (forward) and 5′-GCGTCTAGAtta**ACCCATTTGTTGACCACCTGTCATTGAAGCCAT**gttgacgcggcttttcaaaacatcaagatcc-3′ (reverse) were used to amplify this fragment. The gene-specific sequence is shown in lowercase, and the introduced restriction sites are underlined. T7 epitope tag sequence was added immediately preceding the stop codon TAA and is shown in boldface. The plasmid AtADF1-4Ri for silencing *AtADF1* through *AtADF4* was constructed as illustrated in Supplemental Figure S3, and its design is based on previously published methods (Pawloski et al., 2006).

RNA Isolation and RT-PCR Analysis

Total RNA from leaves was extracted using the RNeasy Plant Mini Kit (Qiagen) and treated with DNA-free (Ambion) to remove contaminating DNA. First-strand cDNA was synthesized from 1 μg of total RNA using SuperScript III reverse transcriptase (Invitrogen). The primers for amplifying *AtADFs* from T-DNA insertional mutants are listed in Supplemental Table S1. The expression of *AtADF* genes was controlled with the Arabidopsis *β-tubulin* gene (National Center for Biotechnology Information accession no. AY059075) using primers 5′-GTCCAGTGTCTGTGATATTGCACC-3′ (forward) and 5′-TTACGAATCCGAGGGAGCCATTG-3′ (reverse). Quantitative RT-PCR was performed on a Mastercycler ep Realplex real-time PCR system as described previously (Ruzicka et al., 2007) using ubiquitin gene *UBQ10* primers (Lai et al., 2004) as the endogenous control. The primers used for *AtADFs*, *PR1* (At2g14610), and *PDF1.2* (At5g44420) are listed in Supplemental Table S2.

Transient Protein Expression in *N. benthamiana* and Laser-Scanning Confocal Microscopy

Transient protein expression in *N. benthamiana* with various plasmids in *Agrobacterium tumefaciens* GV3101 and confocal microscopy using a LSM Zeiss 510 Meta were performed as described previously (Goodin et al., 2002).

Expression and Purification of Recombinant AtADF4

Expression and purification of recombinant AtADF4 from pFLAG-AtADF4 were conducted as described previously (Tian et al., 2004). Protein concentration was calculated using an extinction coefficient of 14,690 M^{-1} cm^{-1} determined with the approach of Gill and von Hippel (1989).

Actin Monomer-Binding Assay

The interaction of AtADFs with actin monomers was examined by measuring the fluorescence change of NBD-labeled ATP- and ADP-loaded G-actin in the presence of varying concentrations of AtADFs as described previously (Chaudhry et al., 2007).

Nucleotide-Exchange Analysis

The rate of nucleotide exchange on 1 μM ATP-G-actin or ADP-G-actin, in physiological or low-salt buffer, was determined by measuring the increase in fluorescence upon incorporation of ε-ATP (Sigma-Aldrich) as described previously (Chaudhry et al., 2007).

Cytochalasin D Treatments

Cytochalasin D (Calbiochem) was dissolved in dimethyl sulfoxide (DMSO) to a concentration of 10 mM. Various solutions containing cytochalasin D (Table I) were prepared by adding appropriate volumes of the stock solution into 10 mM $MgCl_2$ with or without *Pst* (AvrPphB) at 5×10^7 cfu mL^{-1}. For controls, additional DMSO was added to a final concentration of 0.1% where applicable. The infiltration of leaves and observation of the HR were conducted as described above.

Sequence data from this article can be found in the GenBank/EMBL data libraries under accession numbers At5g59890 (ADF4), At5g59880 (ADF3), At3g46010 (ADF1), At2g14610 (PR1), and At5g44420 (PDF1.2).

Supplemental Data

The following materials are available in the online version of this article.

Supplemental Figure S1. RT-PCR analysis of gene expression of *AtADF* genes in wild-type Col-0 and *Atadf* mutant plants.

Supplemental Figure S2. Molecular characterization of transgenic lines of *Atadf4* complemented with *AtADF4* genomic DNA with T7 tag sequence at the C terminus.

Supplemental Figure S3. Oligonucleotides and the procedure to make an RNA interference construct targeting *AtADF1* through *AtADF4* using inverted-repeat PCR (IR-PCR).

Supplemental Table S1. Characterization of null mutants from collected *AtADF4* T-DNA insertion lines.

Supplemental Table S2. Primer sequences of *AtADF*s, *PR1*, and *PDF1.2* used for quantitative RT-PCR.

ACKNOWLEDGMENTS

We thank Elison Blancaflor of The Samuel Roberts Noble Foundation for kindly providing the plasmid ABD2-GFP, and we are grateful to Sheng Yang He, Lindsey Triplett, and members of the Day laboratory (Michigan State University) for critical reading of the manuscript.

Received February 23, 2009; accepted April 1, 2009; published April 3, 2009.

LITERATURE CITED

Ade J, DeYoung BJ, Golstein C, Innes RW (2007) Indirect activation of a plant nucleotide binding site-leucine-rich repeat protein by a bacterial protease. Proc Natl Acad Sci USA **104:** 2531–2536

Aepfelbacher M, Heesemann J (2001) Modulation of Rho GTPases and the actin cytoskeleton by *Yersinia* outer proteins (Yops). Int J Med Microbiol **291:** 269–276

Alfano JR, Collmer A (2004) Type III secretion system effector proteins: double agents in bacterial disease and plant defense. Annu Rev Phytopathol **42:** 385–414

Axtell MJ, Staskawicz BJ (2003) Initiation of RPS2-specified disease resistance in *Arabidopsis* is coupled to the AvrRpt2-directed elimination of RIN4. Cell **112:** 369–377

Burch-Smith TM, Schiff M, Caplan JL, Tsao J, Czymmek K, Dinesh-Kumar SP (2007) A novel role for the TIR domain in association with pathogen-derived elicitors. PLoS Biol **5:** e68

Carlier MF, Laurent V, Santolini J, Melki R, Didry D, Xia GX, Hong Y, Chua NH, Pantaloni D (1997) Actin depolymerizing factor (ADF/cofilin) enhances the rate of filament turnover: implication in actin-based motility. J Cell Biol **136:** 1307–1322

Carlier MF, Ressad F, Pantaloni D (1999) Control of actin dynamics in cell motility: role of ADF/cofilin. J Biol Chem **274:** 33827–33830

Century KS, Holub EB, Staskawicz BJ (1995) NDR1, a locus of *Arabidopsis thaliana* that is required for disease resistance to both a bacterial and a fungal pathogen. Proc Natl Acad Sci USA **92:** 6597–6601

Chaudhry F, Guerin C, von Witsch M, Blanchoin L, Staiger CJ (2007) Identification of *Arabidopsis* cyclase-associated protein 1 as the first nucleotide exchange factor for plant actin. Mol Biol Cell **18:** 3002–3014

Chen CY, Cheung AY, Wu HM (2003) Actin-depolymerizing factor mediates Rac/Rop GTPase-regulated pollen tube growth. Plant Cell **15:** 237–249

Clough SJ, Bent AF (1998) Floral dip: a simplified method for *Agrobacterium*-mediated transformation of *Arabidopsis thaliana*. Plant J **16:** 735–743

Dong CH, Xia GX, Hong Y, Ramachandran S, Kost B, Chua NH (2001) ADF proteins are involved in the control of flowering and regulate F-actin organization, cell expansion, and organ growth in *Arabidopsis*. Plant Cell **13:** 1333–1346

Galan JE, Zhou D (2000) Striking a balance: modulation of the actin cytoskeleton by *Salmonella*. Proc Natl Acad Sci USA **97:** 8754–8761

Gill SC, von Hippel PH (1989) Calculation of protein extinction coefficients from amino acid sequence data. Anal Biochem **182:** 319–326

Goodin MM, Dietzgen RG, Schichnes D, Ruzin S, Jackson AO (2002) pGD vectors: versatile tools for the expression of green and red fluorescent protein fusions in agroinfiltrated plant leaves. Plant J **31:** 375–383

Hao S, August A (2005) Actin depolymerization transduces the strength of B-cell receptor stimulation. Mol Biol Cell **16:** 2275–2284

Hardham AR, Jones DA, Takemoto D (2007) Cytoskeleton and cell wall function in penetration resistance. Curr Opin Plant Biol **10:** 342–348

Holt BF III, Belkhadir Y, Dangl JL (2005) Antagonistic control of disease resistance protein stability in the plant immune system. Science **309:** 929–932

Hussey PJ, Ketelaar T, Deeks MJ (2006) Control of the actin cytoskeleton in plant cell growth. Annu Rev Plant Biol **57:** 109–125

Iriarte M, Cornelis GR (1998) YopT, a new *Yersinia* Yop effector protein, affects the cytoskeleton of host cells. Mol Microbiol **29:** 915–929

Jones JD, Dangl JL (2006) The plant immune system. Nature **444:** 323–329

Kamoun S (2007) Groovy times: filamentous pathogen effectors revealed. Curr Opin Plant Biol **10:** 358–365

Kobayashi Y, Kobayashi I (2007) Depolymerization of the actin cytoskeleton induces defense responses in tobacco plants. J Gen Plant Pathol **73:** 360–364

Kobayashi Y, Kobayashi I, Funaki Y, Fujimoto S, Takemoto T, Kunoh H (1997) Dynamic reorganization of microfilaments and microtubules is necessary for the expression of non-host resistance in barley coleoptile cells. Plant J **11:** 525–537

Kunkel BN, Bent AF, Dahlbeck D, Innes RW, Staskawicz BJ (1993) RPS2, an *Arabidopsis* disease resistance locus specifying recognition of *Pseudomonas syringae* strains expressing the avirulence gene avrRpt2. Plant Cell **5:** 865–875

Lai CP, Lee CL, Chen PH, Wu SH, Yang CC, Shaw JF (2004) Molecular analyses of the Arabidopsis TUBBY-like protein gene family. Plant Physiol **134:** 1586–1597

Li J, Biswas MG, Chao A, Russell DW, Chory J (1997) Conservation of function between mammalian and plant steroid 5alpha-reductases. Proc Natl Acad Sci USA **94:** 3554–3559

Maciver SK (1998) How ADF/cofilin depolymerizes actin filaments. Curr Opin Cell Biol **10:** 140–144

Maciver SK, Hussey PJ (2002) The ADF/cofilin family: actin-remodeling proteins. Genome Biol **3:** reviews3007

Mackey D, Holt BF III, Wiig A, Dangl JL (2002) RIN4 interacts with *Pseudomonas syringae* type III effector molecules and is required for RPM1-mediated resistance in *Arabidopsis*. Cell **108:** 743–754

Mattoo S, Lee YM, Dixon JE (2007) Interactions of bacterial effector proteins with host proteins. Curr Opin Immunol **19:** 392–401

Miklis M, Consonni C, Bhat RA, Lipka V, Schulze-Lefert P, Panstruga R (2007) Barley MLO modulates actin-dependent and actin-independent antifungal defense pathways at the cell periphery. Plant Physiol **144:** 1132–1143

Nimchuk Z, Marois E, Kjemtrup S, Leister RT, Katagiri F, Dangl JL (2000) Eukaryotic fatty acylation drives plasma membrane targeting and enhances function of several type III effector proteins from *Pseudomonas syringae*. Cell **101:** 353–363

Ouellet F, Carpentier E, Cope MJ, Monroy AF, Sarhan F (2001) Regulation of a wheat actin-depolymerizing factor during cold acclimation. Plant Physiol **125:** 360–368

Pawloski LC, Kandasamy MK, Meagher RB (2006) The late pollen actins are essential for normal male and female development in *Arabidopsis*. Plant Mol Biol **62:** 881–896

Pistor S, Chakraborty T, Niebuhr K, Domann E, Wehland J (1994) The ActA protein of *Listeria monocytogenes* acts as a nucleator inducing reorganization of the actin cytoskeleton. EMBO J **13:** 758–763

Ruzicka DR, Kandasamy MK, McKinney EC, Burgos-Rivera B, Meagher RB (2007) The ancient subclasses of *Arabidopsis* actin depolymerizing factor genes exhibit novel and differential expression. Plant J **52:** 460–472

Shao F, Merritt PM, Bao Z, Innes RW, Dixon JE (2002) A *Yersinia* effector and a *Pseudomonas* avirulence protein define a family of cysteine proteases functioning in bacterial pathogenesis. Cell **109:** 575–588

Shen QH, Saijo Y, Mauch S, Biskup C, Bieri S, Keller B, Seki H, Ulker B, Somssich IE, Schulze-Lefert P (2007) Nuclear activity of MLA immune receptors links isolate-specific and basal disease-resistance responses. Science **315:** 1098–1103

Shimada C, Lipka V, O'Connell R, Okuno T, Schulze-Lefert P, Takano Y (2006) Non-host resistance in *Arabidopsis-Colletotrichum* interactions acts at the cell periphery and requires actin filament function. Mol Plant Microbe Interact **19:** 270–279

Simonich MT, Innes RW (1995) A disease resistance gene in *Arabidopsis* with specificity for the avrPph3 gene of *Pseudomonas syringae* pv. *phaseolicola*. Mol Plant Microbe Interact **8:** 637–640

Skalamera D, Heath MC (1998) Changes in the cytoskeleton accompanying infection-induced nuclear movements and the hypersensitive response in plant cells invaded by rust fungi. Plant J **16:** 191–200

Staiger CJ, Blanchoin L (2006) Actin dynamics: old friends with new stories. Curr Opin Plant Biol **9:** 554–562

Stamnes M (2002) Regulating the actin cytoskeleton during vesicular transport. Curr Opin Cell Biol **14:** 428–433

Takemoto D, Hardham AR (2004) The cytoskeleton as a regulator and target of biotic interactions in plants. Plant Physiol **136:** 3864–3876

Takemoto D, Jones DA, Hardham AR (2003) GFP-tagging of cell components reveals the dynamics of subcellular re-organization in response to infection of *Arabidopsis* by oomycete pathogens. Plant J **33:** 775–792

Thomas P, Schiefelbein J (2002) Cloning and characterization of an actin depolymerizing factor gene from grape (*Vitis vinifera* L.) expressed during rooting in stem cuttings. Plant Sci **162:** 283–288

Tian M, Huitema E, Da Cunha L, Torto-Alalibo T, Kamoun S (2004) A Kazal-like extracellular serine protease inhibitor from *Phytophthora infestans* targets the tomato pathogenesis-related protease P69B. J Biol Chem **279:** 26370–26377

Tornero P, Dangl JL (2001) A high-throughput method for quantifying growth of phytopathogenic bacteria in *Arabidopsis thaliana*. Plant J **28:** 475–481

Wang YS, Motes CM, Mohamalawari DR, Blancaflor EB (2004) Green fluorescent protein fusions to *Arabidopsis* fimbrin 1 for spatio-temporal imaging of F-actin dynamics in roots. Cell Motil Cytoskeleton **59:** 79–93

Yu IC, Parker J, Bent AF (1998) Gene-for-gene disease resistance without the hypersensitive response in *Arabidopsis* dnd1 mutant. Proc Natl Acad Sci USA **95:** 7819–7824

Yun BW, Atkinson HA, Gaborit C, Greenland A, Read ND, Pallas JA, Loake GJ (2003) Loss of actin cytoskeletal function and EDS1 activity, in combination, severely compromises non-host resistance in *Arabidopsis* against wheat powdery mildew. Plant J **34:** 768–777

Zhao Y, Thilmony R, Bender CL, Schaller A, He SY, Howe GA (2003) Virulence systems of *Pseudomonas syringae* pv. *tomato* promote bacterial speck disease in tomato by targeting the jasmonate signaling pathway. Plant J **36:** 485–499